Electronic Supplementary Material (ESI) for Nanoscale.

Ruptured Liquid Metal Microcapsules Enabling Hybridized Silver Nanowire Networks Towards High-Performance Deformable Transparent Conductors

Shipeng Wang[1¶], Huaisen Tian[1¶], Yawen Wang[2], Haojie Zuo[2], Chengliang Tao[1], Jiawei Liu[1], Pengyuan Li[1], Yan Yang[1], Xu Kou[1], Jiangxin Wang[1], Wenbin Kang[2*]*

[1] School of Mechanical Engineering, Sichuan University, Chengdu 610065, China
[2] State Key Laboratory of Environment-Friendly Energy Materials, Southwest University of Science and Technology, Mianyang, 621010, China

[¶] These authors contributed equally to this manuscript

[*] Corresponding Email: wenbin.kang@swust.edu.cn; wangjiangxin@scu.edu.cn

Supplementary Information

Table S1 List of representative welding treatment methods

Method	Features	R_s (ohm sq^{-1}), before	R_s (ohm sq^{-1}), after	T (%)	Transfer-free	Mechanical and Chemical Enhancement	Ref
Heat treatment	Low consumption, fast, precise temperature control, unsuitable for heat-sensitive substrates	30	10	85	N	N	1
Chemically welding	Energy-saving, large-scale fabrication, adding additional material	7.06×10^{3}	11.2	72	N	N	2
Plasmonic treatment	Low temperature, fast, specialized equipment	120	19	98	N	N	3
Mechanical pressing	Cold welding, simple, high pressure, damage to the device structure	1.8×10^{4}	8.6	-	N	N	4
Capillary-force-induced welding	Room temperature, simple, efficiently, specific hydrophobic substrates and solution viscosities	7×10^{3}	150	83	N	N	5
Laser nano-welding	Fast-process, efficiently, expensive equipment, unsuitable for large-scale manufacturing	87	25	94	N	N	6
Atomic layer deposition	Specific equipment, complex process conditions, unsuitable for large-scale manufacturing	75	9	72	Y	-	7
This work	Room temperature, fast, energy-saving	132	10	74	Y	Y	

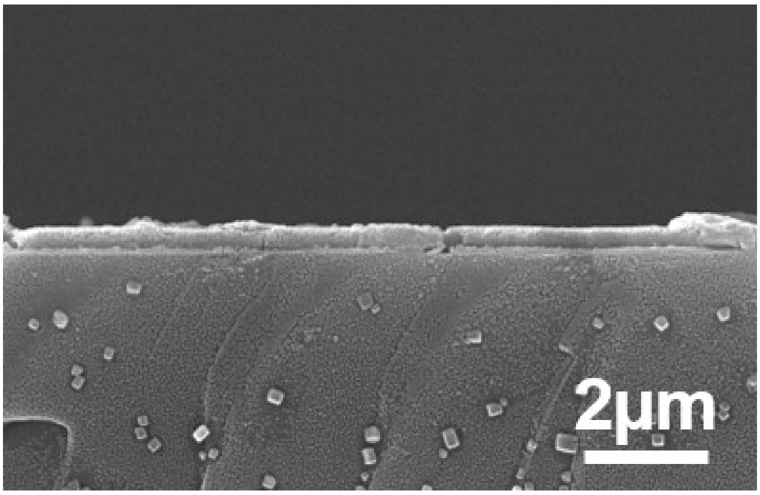

Fig. S1. The SEM image of the cross-sectional view of the electrode to identify the thickness of the liquid metal overlay.

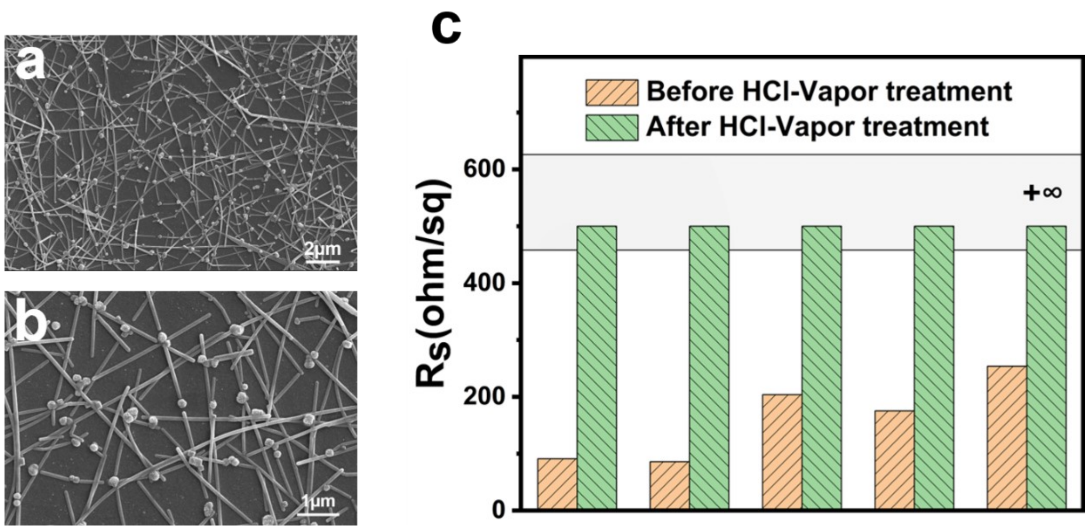

Fig. S2. (a, b) SEM images of AgNWs network after HCl-vapor treatment. (c) The sheet resistance of AgNWs network before and after HCl-vapor treatment.

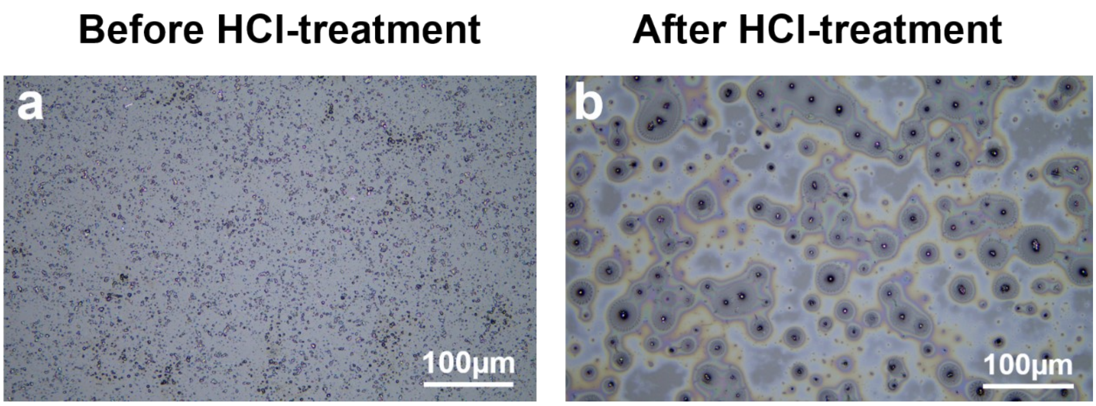

Fig. S3. (a) LMMs distributed on glass substrate before HCl-vapor treatment. (b) LMMs distributed on glass substrate after HCl-vapor treatment.

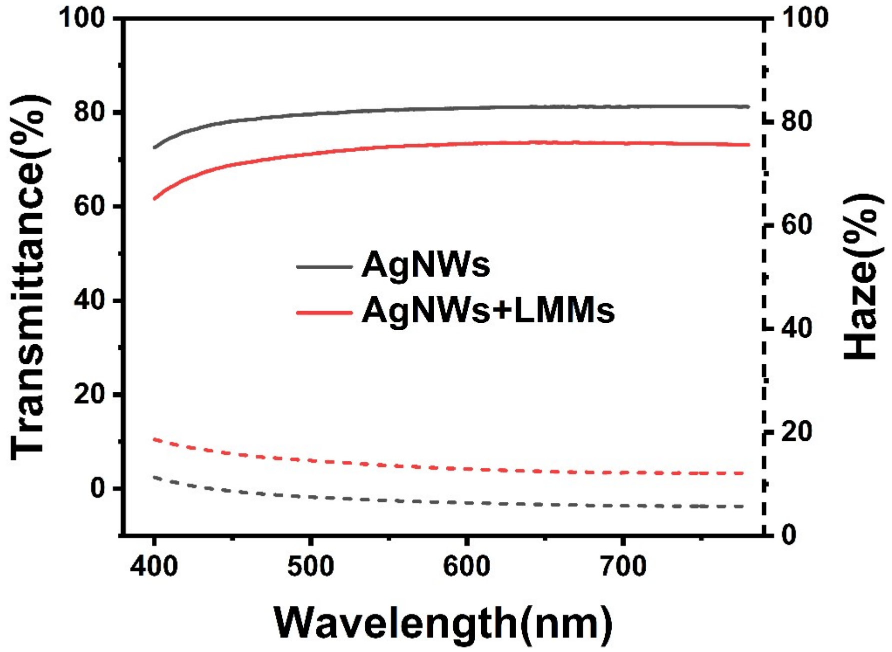

Fig. S4. Transmittance and haze curves of transparent conductors before and after spraying LMMs.

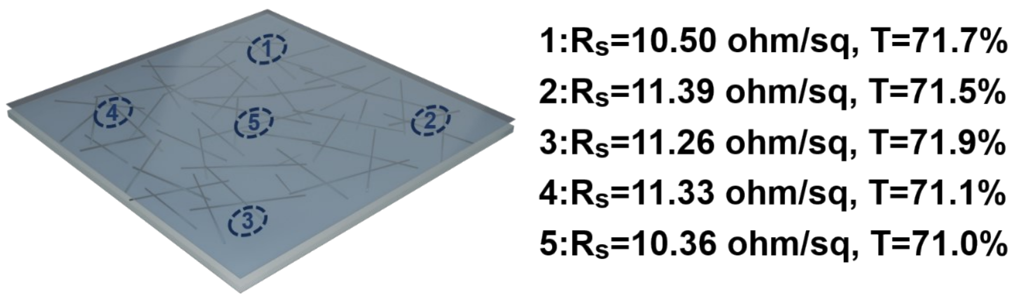

Fig. S5. Sheet resistance and transmittance at different positions of AgNWs-LM conductor.

Table S2 List of sheet resistances of the samples for testing

Testing name	Figure number	Sheet resistance (ohm sq^{-1})
chemical stability testing	Fig 2d	10~15
tape testing	Fig 2e	8.34
ultrasound testing	Fig 2f, Fig 2g	11.48 and 12.39
cyclic bending test	Fig 2h	12.74
comparison test with ITO	Fig 2i	18.65
The strain sensor	Fig 4	10~15

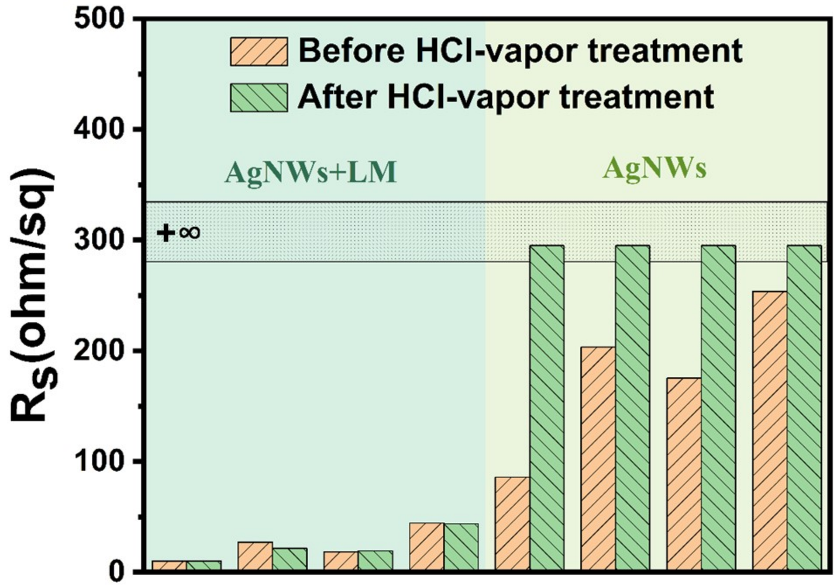

Fig. S6. The sheet resistance of AgNWs-LM conductor and AgNWs network before and after HCl-vapor treatment.

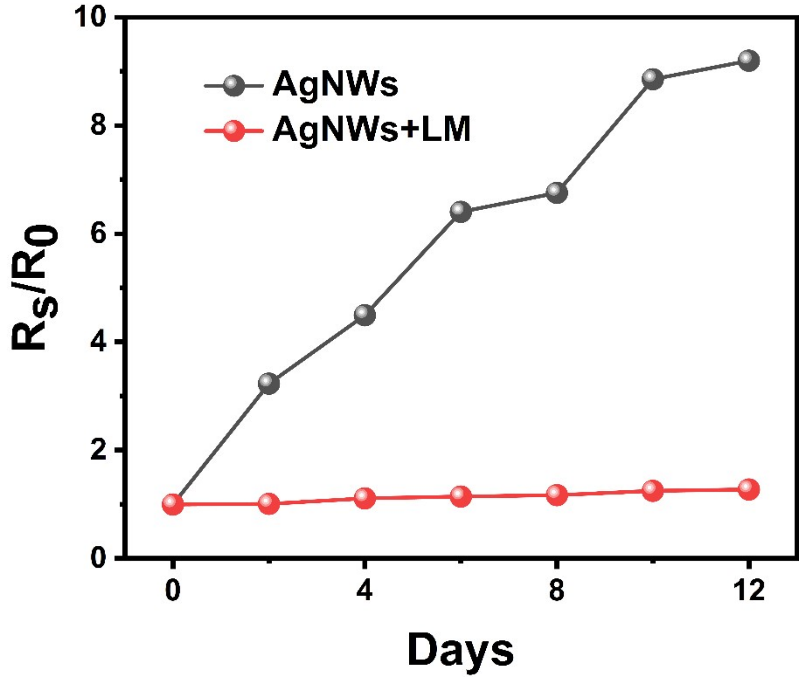

Fig. S7. Conductivity stability of AgNWs-LM and AgNWs conductors in ambient air.

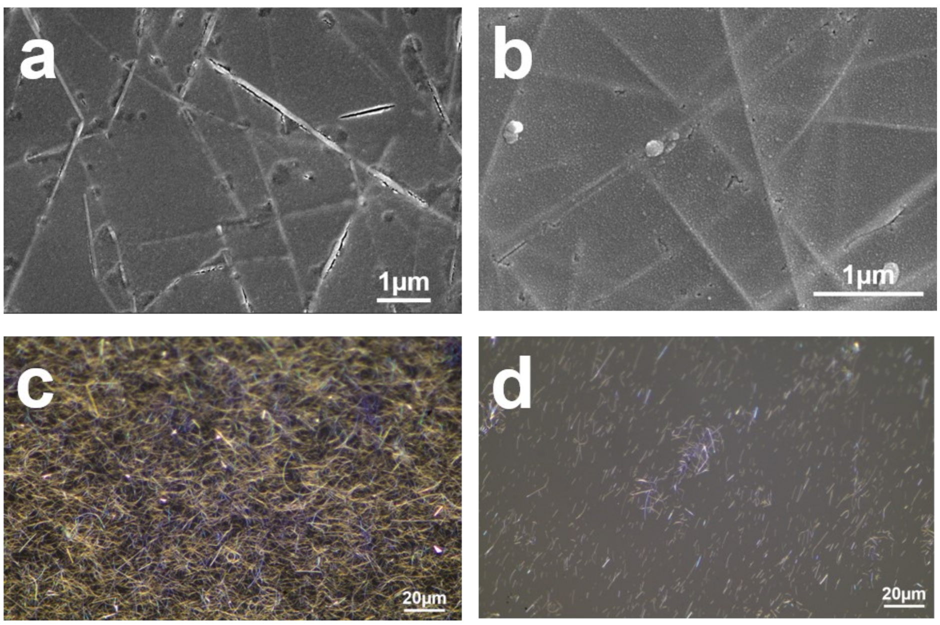

Fig. S8. (a, b) The SEM images of the surface of AgNWs-LM conductor before and after adhesion test. (c, d) The optical microscope images of the surface of AgNWs networks before and after adhesion test.

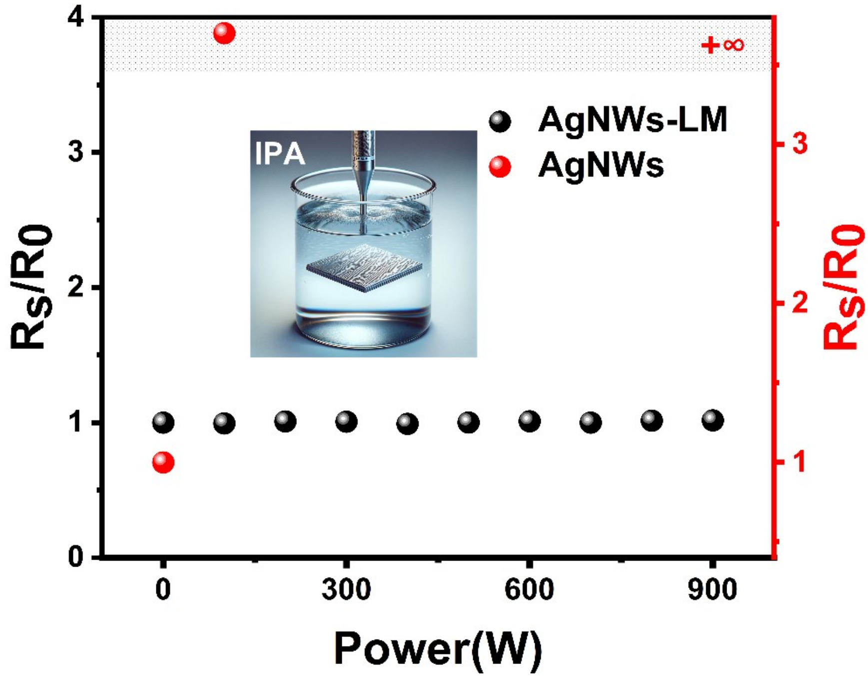

Fig. S9. The sheet resistance variation of the AgNWs-LM conductor after 60 seconds of ultrasonic treatment at varying power levels in IPA.

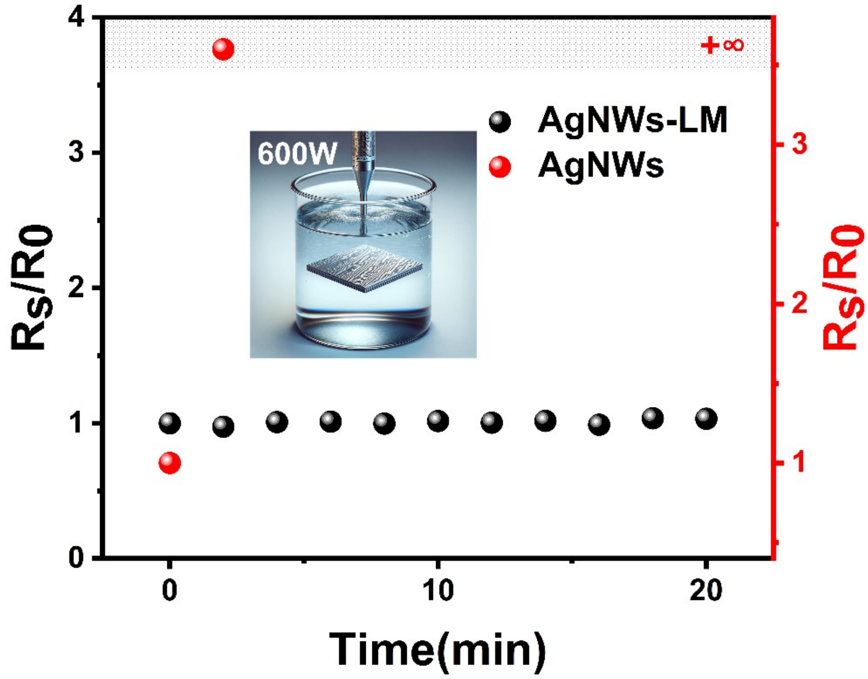

Fig. S10. The sheet resistance variation of the AgNWs-LM conductor under 600 W ultrasonic treatment in 20 mins in IPA.

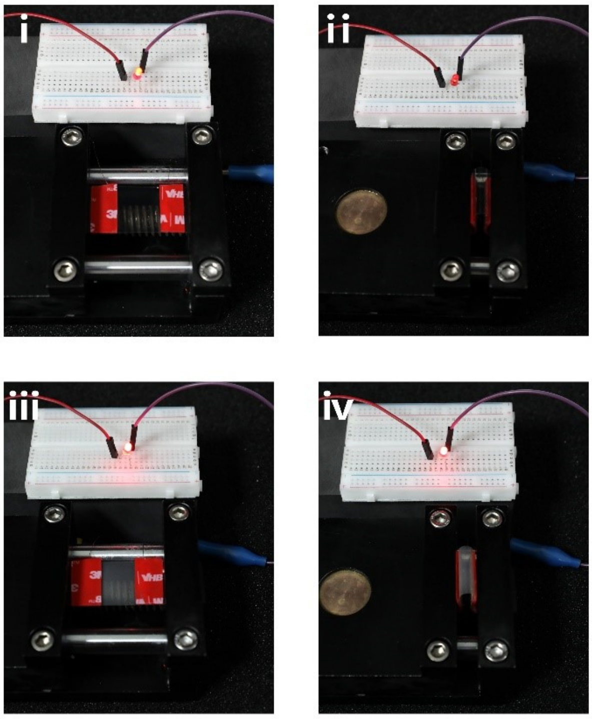

Fig. S11. Photographs of a powered LED integrated with the ITO and AgNWs-LM conductor under different bending radius.

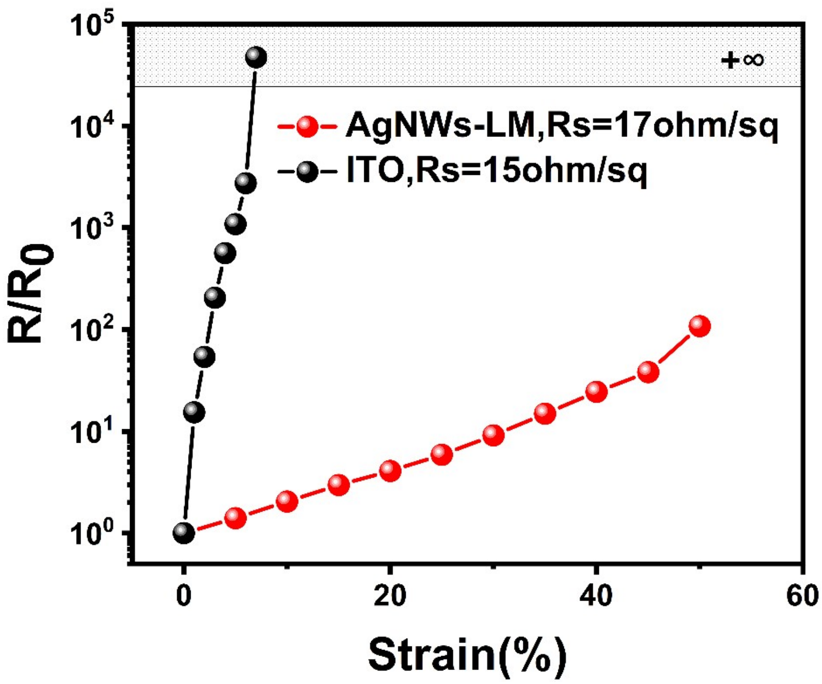

Fig. S12. The resistance changes of ITO and AgNWs-LM conductor under stretching.

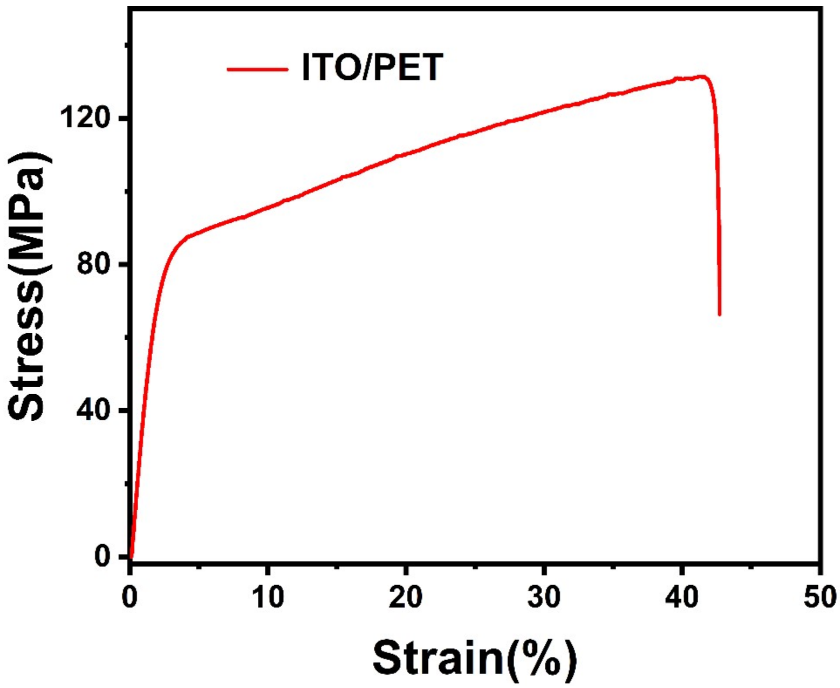

Fig. S13. The stress-strain curve of ITO/PET.

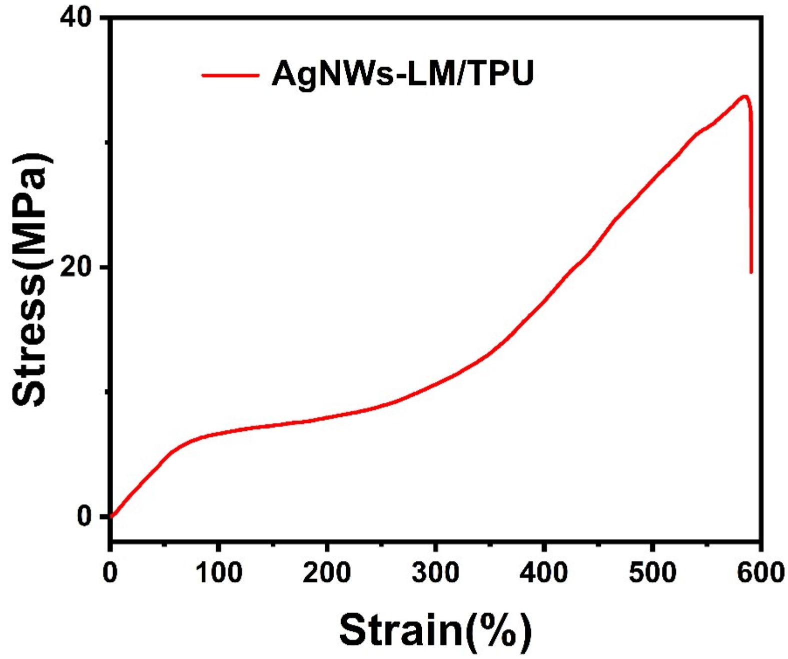

Fig. S14. The stress-strain curve of AgNWs-LM/TPU.

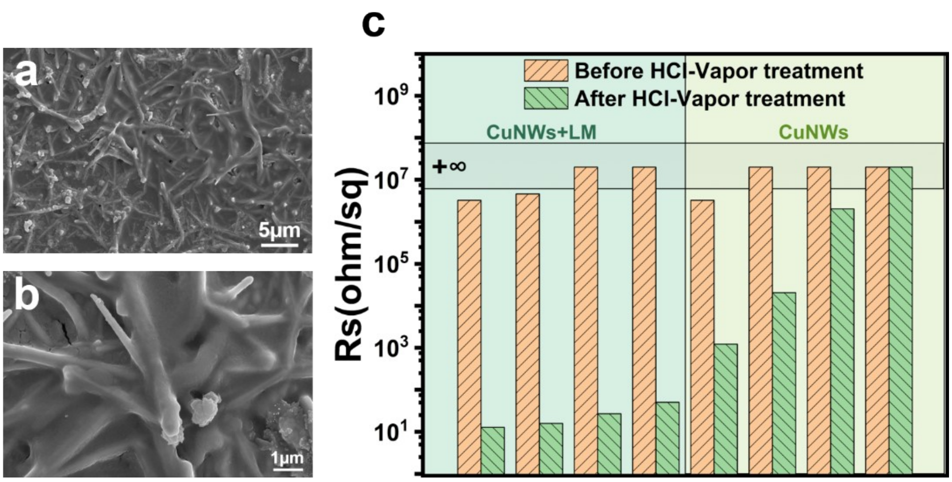

Fig. S15. (a, b) SEM images of liquid metal wetted with copper nanowires after HCl-vapor treatment. (c) Sheet resistance of CuNWs-LM conductor and CuNWs network before and after HCl-vapor treatment.

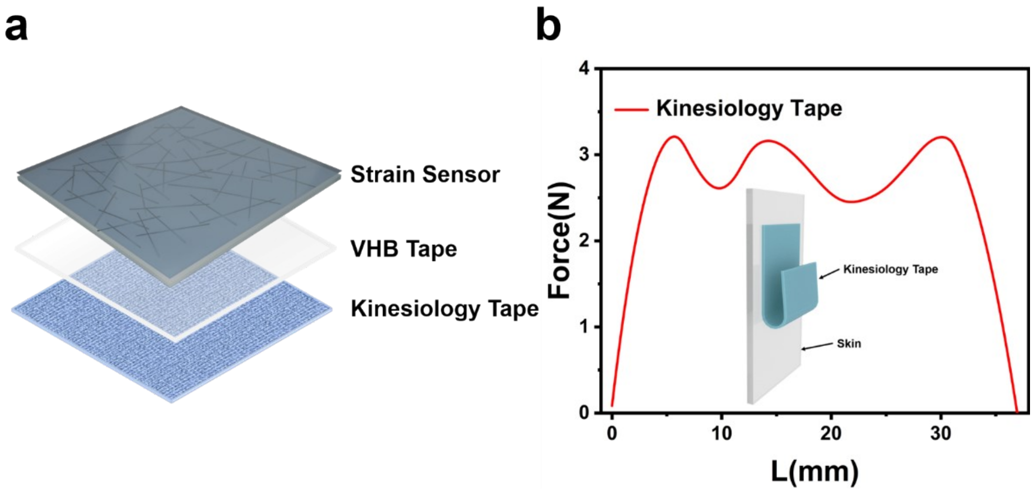

Fig. S16. (a) The structure of the strain sensor. (b) The peel test curve of kinesiology tape.

References

1. A. Teymouri, S. Pillai, Z. Ouyang, X. Hao, F. Liu, C. Yan and M. A. Green, *ACS Appl. Mater. Interfaces*, 2017, **9**, 34093-34100.
2. L. Lian, X. Xi, D. Dong and G. He, *Org. Electron.*, 2018, **60**, 9-15.
3. J. H. Park, G. Hwang, S. Kim, J. Seo, H. Park, K. Yu, T. Kim and K. J. Lee, *Adv. Mater.*, 2017, **29**, 1603473.
4. T. Tokuno, M. Nogi, M. Karakawa, J. Jiu, T. T. Nge, Y. Aso and K. Suganuma, *Nano Res.*, 2011,

4, 1215-1222.
5. Y. Liu, J. Zhang, H. Gao, Y. Wang, Q. Liu, S. Huang, C. F. Guo and Z. Ren, *Nano Lett.*, 2017, **17**, 1090-1096.
6. J. Ha, B. J. Lee, D. J. Hwang and D. Kim, *RSC Adv.*, 2016, **6**, 86232-86239.
7. Y. Weng, G. Chen, X. Zhou, Y. Zhang, Q. Yan and T. Guo, *J. Mater. Sci.*, 2023, **58**, 17816-17828.